IOP Publishing Physica Scripta
Phys. Scr. 95 (2020) 055605 (11pp) https://doi.org/10.1088/1402-4896/ab5ab2

Rocket effect on dust particles in the tokamak SOL

E Lazzaro, G Gervasini, F Ghezzi, A Uccello and JET contributors[1]

Istituto per la Scienza e Tecnologia dei Plasmi-CNR, Via R. Cozzi 53, I-20125 Milan, Italy

E-mail: lazzaro@ifp.cnr.it

Received 11 July 2019, revised 16 October 2019
Accepted for publication 22 November 2019
Published 2 March 2020

Abstract

An accurate study of the motion of particles of variable mass and charge, in interaction with the SOL plasma, requires considering in the dynamic model, all the effects of the same order of magnitude. Here we present an extension of the conventional point-like particle model introducing a discussion of the rocket acceleration consequent to the asymmetric mass evaporation of a particle traveling in the SOL. A simplified but realistic description of the asymmetric loss of mass is constructed in analogy with the physics of comets.

Keywords: dust, tokamak, SOL, rocket acceleration, evaporation

(Some figures may appear in colour only in the online journal)

1. Introduction

In association with vertical disruption events in tokamaks, significant melting along tile ridges of the vessel upper dump plate has often been observed, over the whole width with release of metallic particulate and droplets [1–3]. In the context of the interent on research on dust transport, going on at the Joint European Torus (JET) [4], here we propose a contribution on a particular problem of dust dynamics. An accurate study of the motion of these particles, of variable mass and charge, in interaction with the SOL plasma, requires considering in the dynamic model, all the effects of the same order of magnitude. With full awareness that the problem cannot be solved strictly self-consistently, mainly because of the geometric uncertainties and complexities of thermodynamic transformations in flight in the harsh SOL environment, here we propose an investigation which isolates key aspects and paradigmatic behavior of dust grains and droplets in a smooth ablation regime, without sudden disintegration. Basically we present an extension of the conventional point-like particle model, introducing a discussion of the additional acceleration consequent to the asymmetric mass evaporation of a particle traveling in the SOL. The basic mechanism is due do the asymmetric heating and consequent asymmetric mass ejection in the direction opposite to the impinging heat flux, by sublimation, when the temperature is below melting,and vaporization when a phase transition to liquid state is entered, still remaining below boiling. The main objective of the work is to assess the magnitude, the direction and the scaling of the 'rocket force' acting on micrometric particulate of the metallic elements prevalent in the debris of a tokamak wall, with a focus on the case of Beryllium and composites, which are of interest in fusion oriented experiments. A simplified but realistic description of the asymmetric loss of mass is constructed in analogy with the physics of comets [5–11] to obtain an applicable model for dust tracing codes dealing with pointlike particles. Through numerical tests in mock-up tokamak situations an assessment is obtained of the range of parameters where the rocket acceleration may be relevant. In the next sections the work is organized with the following logic: (i) isolating the key aspect of the dynamics of a body which in flight loses mass asymmetrically. (ii)Develop from geometric similarity a point-like dust model (presently applied in all trajectory codes) which retains the essential characteristics of a finite size particle (see figure 1). (iii) Consider initially for the sake of principle, the simplest, idealized 'environment' and interactions: vacuum and gravity (iv) consider subsequently the simplest 'tokamak-like' environment with the relevant interactions: B field and gravity, and mock-up of drag force.

2. Mass loss of dust particles in the tokamak SOL

The dominant forces on dust particles traveling in the tokamak SOL are the ion and neutral drag forces, gravity and to a

[1] See Joffrin *et al* (DOI:10.1088/1741-4326/ab2276) for the JET contributors.

 © Consiglio Nazionale delle Ricerche Printed in the UK

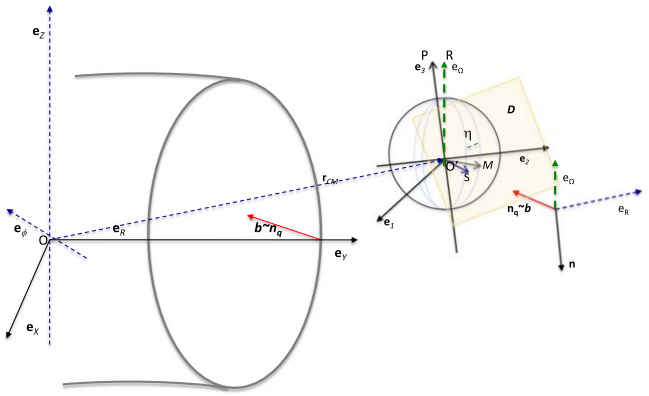

Figure 1. A schematic picture (not to scale) of a finite size spherical rotating particle in the SOL of a tokamak, in the cylindrical coordinate system R, ϕ, Z. Here O' is the center of the particle core in its intrisic reference frame $\mathbf{e}_1$, $\mathbf{e}_2$, $\mathbf{e}_3$.The axis $\overline{O'R}$ is the instantaneous rotation axis and $\overline{O'P}$ is tangent to the particle trajectory; $\overline{O'S}$, is a generic illuminated point on the day side (D) of a plane perpendicular to the heat flux direction $\mathbf{n}_q$. In principle a generic illumination point at S, and the site of the maximum outgassing at M are separated by an angular lag η vanishing as the surface temperature gets more nuniform, on a timescale presumably longer than the particle spin time, so that $\overline{SO'}$ is in the direction of the heat flux vector from the SOL, oblique (often nearly perpendicular) to the particle trajectory $\mathbf{n}$ and nearly parallel to the magnetic field lines $\mathbf{b}$. $\overline{O'M}$ indicates the axis of a conic volume of ejected mass: in the limit $\eta \propto \frac{\delta^2}{a_d^2} \to 0$, $\overline{O'S}$ and $\overline{O'M}$ are aligned.

lesser extent, electric fields [12, 13]. In addition, the heat flux impinging on the particle is the cause of asymmetric sublimation/evaporation, with loss of mass in flight, driving a rocket force. The rate of sublimated/evaporated mass ejection, and the magnitude of its speed can be estimated from established gas dynamic laws, but for application to micrometric particles traveling in the very low pressure SOL environment some attention is required in applying appropriate and up-to-date evaporation/sublimation models. The magnitude of the 'rocket' acceleration, proportional to the mass loss rate, depends crucially on the dust particle temperature. The mass M_d of a spherical particle, of initial radius a_d, traveling in the SOL of a tokamak varies as:

$$\frac{\mathrm{d}M_d}{\mathrm{d}t} = 4\pi a_d^2\left[\sum_r m_r\Gamma_{r,\mathrm{in}} - \sum_s m_s\Gamma_{s,\mathrm{out}}\right] \ (\mathrm{kg\ s^{-1}}) \qquad (1)$$

due to incoming molecular mass fluxes of ions and neutrals and outflux of dust particles due to basic and radiation enhanced sublimation processes, physical and chemical sputtering,reflected atoms and ions previously absorbed and later released [12–14]. Here m_s are the atomic masses. For the objectives of this paper here it is sufficient to consider a simplified description,compared with that outlined in [12]. The hydrogen concentration on the dust surface is saturated so influx and outflux of hydrogen are balanced, while the net ionic flux from impurities contributes to particle mass flux. So the total mass flux reduces to the net difference between incoming and outgoing impurity fluxes. For definiteness, here we focus on the dominant mechanism of mass loss which is sublimation/evaporation, in the temperature regime of a particle in flight. The dominating sublimated mass flux leads to fast radius/mass reduction for temperatures near the dust material above melting temperature. In the present investigation all the contributions in equation (1), are lumped in a, temperature dependent, sublimation/evaporation term. Consequently, in the context of fully operating dust trajectory codes for isolated macroscopic dust particles, in order to isolate the mechanical effects of mass ejection, it is sufficient to have information on the instantaneous thermodynamic state of the particle, close to the solid–gas or liquid–gas state transition. For a dust particle moving in the tokamak SOL, the basic concepts are to be found in the established theory of evaporation [15–23] and other important elements can be borrowed from the outgassing model of a comet [5–11].

3. Evaporation and sublimation mass flux from metallic droplets

A short review of the concepts of evaporation theories helps in the correct application to our problem. A schematic model of the sublimating/evaporating particle should consider at least a two phase system, solid-vapor or liquid-vapor. In general such a system is in dynamic equilibrium, since for every value of surface temperature there are two fluxes that are equal and in opposite directions: Γ_L is the unidirectional evaporation flux *from* the liquid phase across the interface, and Γ_V is the unidirectional condensation flux in the direction from the vapor phase *towards* the interface. We focus now, for clarity, on case with temperature up to and slightly above the melting value T_i^L, at the inteface i, assuming a negligibly low ambient pressure. For convenience in checking evaluations of the formulae, we specify the definitions and units in the appendix B. Under the assumption that the Maxwell–Boltzmann particle distribution is applicable, the mass outflux is often expressed as the Hertz–Knudsen–Langmuir law [17, 19–22]:

$$\Gamma_{\mathrm{HKL}} = \sigma_e p_s(T_i^L)\sqrt{\frac{M}{2\pi R T_i^L}} - \sigma_c p_{\mathrm{eq}}\sqrt{\frac{M}{2\pi R T_i^{\mathrm{eq}}}} \quad (\mathrm{kg\ m^{-2}s^{-1}}), \qquad (2)$$

where $p_s(T_i^L)$ is the saturation-vapor pressure at the liquid-vapor interface labeled i, at the temperature T_i^L, of the liquid at phase transition, and p_{eq} is the *'equilibrium'* vapor pressure of the vapor-liquid coexistence ($T_i^{\mathrm{eq}} = T_i^L$), far from the interface [20, 21]; σ_e, σ_c are the evaporation and condensation coefficients respectively [15, 17–22]. The latter coefficients, ranging between 0 and 1 represent the fraction of particles that strike the interface and change phases from their initial liquid or vapor thermodynamic state, respectively, and therefore they represent the ratio of the 'actual' unidirectional flux compared to the maximum flux predicted from classical kinetic theory [17–20, 22]. According to [19, 22], for curved evaporating surfaces, as is the case of small droplets, the coefficients σ_e, σ_c are close to unity. When there is a net free

Table 1. Coefficients of expression for the vapor pressure of Be.

State	*A*	*B*	*C*	*D*
(I) Solid [15]	6.186	1.454×10^{-4}	−16734	0
(II) Solid [16]	8.042	−0.444	−17020	0
(III) Liquid [16]	5.786	0	−15731	0

molecular outflow (net evaporation rate), since the velocity distributions of molecules incoming and outgassing on the *L–V* interface would be different, the evaporating or condensing molecules should be described *at least* by a Maxwellian velocity distribution shifted by a mean (outflow) velocity [18–20, 23]. This leads to the Hertz–Knudsen–Schrage modified expression [19, 21, 22] obtained from equation (2) replacing $\sigma_e = \sigma_c$ with an effective evaporation coefficient $\eta = 2$ for the flux which turns out to be twice that predicted by the Hertz–Knudsen formula.

Following the arguments of Safarian [20, 24], the pressure $p_{\rm eq}$ in equation (2) should be replaced by the *effective vacuum pressure* $p_{\rm eff} = \frac{p_s(T_i^L)}{(1.22 + 3.95\,/\,\eta)} \approx 0.278 p_s(T_i^L)$, for an evaporation coefficient $\eta = 1.667$ and consistent with a subsonic flux. Consequently the mass flux can be expressed as:

$$\Gamma_m = \alpha p_s(T_i^L)\sqrt{(M/2\pi R T_i^L)} \;\; (\mathrm{kg\ m^{-2}\ s^{-1}}) \tag{3}$$

with an *accomodation* factor $\alpha \approx \eta(1 - p_{\rm eq}/p_s)$ which plays the role of an effective evaporation coefficient [20, 21], in the range $0.844 < \alpha < 1.667$. For use in the formula above, pressure must be expressed in (Pa). Actually evaporating particles in a tenuous tokamak SOL environment,with $p_{\rm eq} \ll p_{\rm eff}$, find 'open system' conditions close to vacuum,deviating from mass equilibrium, where the mass in vapor phase can be considered lost [20, 21] . Furthermore,along the lines of [17, 19, 20], here we adopt the following estimate of the mass ejection mean velocity (relative to the C.M.), when there is no condensation:

$$V_{\rm out} \approx \frac{8}{9}\sqrt{\frac{RT_i^L}{2\pi M}} = \widehat{M}_{\rm Mach} C_s \;\; (\mathrm{m\ s^{-1}}), \tag{4}$$

where C_s is the sound speed (at the corresponding vapor density),with $\widehat{M}_{\rm Mach}$ the Mach number. The sublimation /evaporation pressure is related to the surface temperature by the Clausius–Clapeyron relation:

$$p_s(T) = p_s(T_i^L)\mathrm{e}^{-\frac{\Delta H_s}{N_{\rm A} k_B}\left[\frac{1}{T} - \frac{1}{T_i^L}\right]}, \tag{5}$$

where $\Delta \mathrm{H_s}$ is the sublimation/evaporation enthalpy and $N_{\rm A}$ Avogadro's number. In practice, empirical formulas based on experimental data [15, 16] are more useful to find the vapor pressure of an element

$$\log(p_s(\mathrm{atm})) \simeq A + B \cdot \log(T) + C/T + D/T^3. \tag{6}$$

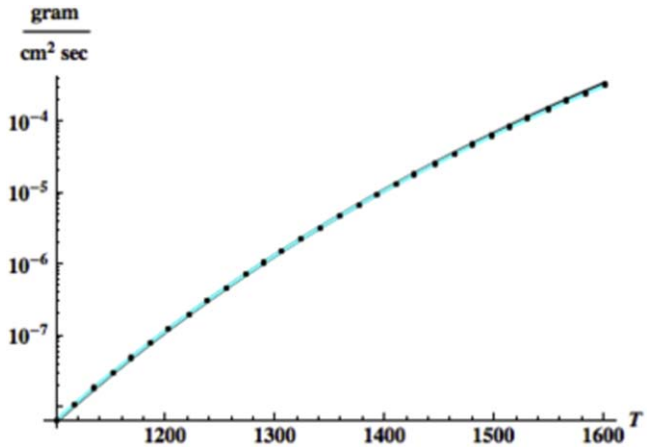

Figure 2. Benchmark of the mass flux (g cm^{-2} s^{-1}) calculations, ([17, 20] (black markers), [15](cyan line))) with the Be evaporation study of [15] in range 1100 °K $< T <$ 1600 °K.

In table 1 we report for convenience of the reader the actual coeffcients used in this work for two thermodynamic states of Be. For the example of solid Beryllium of interest here, up to 1552 °K the coefficients (I) are used, from the historical source useful for benchmarking [15]; in the next interval up to 1800°K the coefficients used are (II). Finally, beyond the third line (III) should be used, although this regime turns out to be too extreme .

Under the assumptions made, from expressions (3), (4) and (6) we can assemble the rate of the outflux Γ_Q of momentum density Q (kg m^{-2} s^{-1}), which turns out to be just proportional to the vapor pressure at the liquid-vapor interface:

$$\frac{\mathrm{d}\Gamma_Q}{\mathrm{d}t} = \xi \widehat{M}_{\rm Mach}\frac{p_s(T_i^L)}{2\pi} \;\; (\mathrm{kg\ m^{-1}\ s^{-2}}), \tag{7}$$

where $\xi \ll 1/2$ is an asymmetry factor discussed later. Expression (7) is consistent with recent detailed numerical investigations [21, 25] in a wider context, and can be retrieved in the general theoretical formulations such as [17, 19, 20, 23]. This gives the basis for estimating the order of magnitude of the rocket force acting on the particle. For the validation of (7) used in the present work, the expressions (2), (4), (7) have been benchmarked against the data of Holden [15] as shown in figure 2. In table 2 a summary is presented of the values of mass evaporation and outgassing speed in the different thermodynamic states of table 1

For the purpose of constructing an applicable model while retaining most of the physics, it is convenient to start considering a finite size spherical particle reaching eventually a limit description for a point-like object. In order to find the vector direction of this force in this limit, suitable definitions must be given of the heat flow direction vector $\mathbf{n}_q$ and trajectiory direction vector $\mathbf{n}$, in terms of which the 'dayside' and 'nightside' of the particle can be identified by a label referring *just* to the side of the trajectory facing the incoming heat flux, here associated mainly with the convective ion contribution.

Table 2. Typical evaporation values.

T_s (°K)	p_s (Pa)	ρ_s (kgm^{-3})	$V_{\rm out}$ (m s^{-1})	Γ_m (kg m^{-2} s^{-1})
1552 (I)	4.8	3.225×10^{-6}	424	0.00 1368
1560 (I)	5.2446	3.6443×10^{-6}	425.4	0.001 4532
2742 (III)	1.13×10^5	4.483×10^{-2}	634.5	25.28

4. Dynamic effects due to mass evaporation

The Newton and angular momentum balance equations relevant to a body which ejects mass while in motion, are [26]:

$$M_d \frac{\mathrm{d}\mathbf{v}}{\mathrm{d}t} = \mathbf{R} - \frac{\mathrm{d}M_d}{\mathrm{d}t}\mathbf{v}_{\rm rel}, \tag{8}$$

$$\boldsymbol{\sigma} \cdot \frac{\mathrm{d}\boldsymbol{\omega}}{\mathrm{d}t} + \boldsymbol{\omega} \wedge \boldsymbol{\sigma} \cdot \boldsymbol{\omega} = \mathbf{T} + \frac{\mathrm{d}M_d}{\mathrm{d}t}\mathbf{r} \wedge \mathbf{v}_{\rm rel}. \tag{9}$$

Here M_d is the mass of a (initially spherical) dust grain of radius a_d, $\mathbf{R}$ and $\mathbf{T}$ are the resultants of all other external forces and torques, ω is the angular velocity vector, $\mathbf{v}_{\rm res} = \mathbf{v}_{\rm out} - \mathbf{v}_{\rm CM}$ the outgassing velocity relative to the center of mass (CM) speed $\mathbf{v}_{\rm CM}$, $\boldsymbol{\sigma}$ the tensor of inertia, which *for a sphere* reduces to $\boldsymbol{\sigma} = \frac{2}{5}M_d a_d^2 \mathbf{I}$; in this case the second term on the left-hand side of equation (9) is identically null. On the right hand side $\mathbf{r}$ is the position vector from a reference origin O in the SOL to the CM of the spherical particle. The effect of asymmetric outgassing, with higher mass ablation from the dayside, consists in the so called Tsiolkovski rocket force:

$$\mathbf{F}_{\rm rock} = -\mathbf{v}_{\rm rel}\frac{\mathrm{d}M_d}{\mathrm{d}t}. \tag{10}$$

The loss of mass is expected to be anisotropic since the sublimation/evaporation is higher on the more intensely heated half surface of the particle (initially spherical) facing the plasma heat flux. The main problem addressed here is the determination of its scalar value and vector direction in the tokamak environment and on the basis of the conditions of heating and outgassing. The second equation of the cardinal system (8), (9) shows that associated with this force there is a torque, causing an intrinsic spin and orbital twist. A more refined model should consider the particle non-spherical deformation, with the evolution of the (ellipsoidal) major axis, as done for comets dynamics. Our model, with suitable simplifications and in the limit of a point-like particle, aims at determining the scaling and direction of the rocket force in the SOL just in relation with the particle CM trajectory, with respect to the main heat flux source from the plasma. The question of the direction of the application of the force relative to that of the trajectory $\mathbf{n} = \mathbf{v}/|v|$ is addressed in the next section.

5. Comet model of asymmetric mass loss

5.1. Geometrical conditions

In the tokamak environment, it is not immediately obvious which is the direction of the force. Here we address the problem of determining the direction of application of the rocket force to a point like particle, as a limiting case of the mechanics of a macroscopic body, such as a comet, partially exposed to the heating on the Sun facing side. Our approach is to start with the cardinal equations of mechanics of a finite size rigid (spherical) body with variable mass and subsequently pass to the limit of a point-like particle. The body (labeled S) is assumed to consist of a solid core (labeled S_s) of constant mass and a portion S_v of variable mass,consisting in a thin outer layer of thickness $\delta \ll a_d$; $S = S_s \cup S_v$. The geometry of the problem is shown in figure 1 and described in the appendix A, inspired by [5, 6, 11].

The model of outgassing of a 'snowball' comet [5–11] provides useful elements for the case of a dust particle moving in the tokamak SOL.We have to consider the direction vector $\mathbf{n}$ tangent to the particle trajectory, parallel to the CM velocity direction $\mathbf{v}_{\rm CM}/v_{\rm CM}$, and the incident heat flux $\mathbf{n}_q = \mathbf{q}/q$. In the tokamak case, referring to the main (R, ϕ, Z) coordinate system,with major radius R_0 and with the basic magnetic field structure $\mathbf{B} = B_\phi \mathbf{e}_\phi + B_\vartheta \mathbf{e}_\vartheta$,the plasma heat flux vector in the SOL is $\mathbf{q} = q_{//}(R, Z)\mathbf{b} + \mathbf{q}_\perp(R, Z)$, with the ordering $q_\perp/q_\parallel \ll 1$. Therefore using $\mathbf{b} = e_\phi + \frac{B_\vartheta}{B}e_\vartheta$ we get $\mathbf{n}_q = \frac{q_{//}}{q}\left[e_\phi + \frac{B_\vartheta}{B}e_\vartheta\right] + \frac{q_\perp}{q}\mathbf{n}_\perp$ where $\vartheta = \arctan[Z/(R - R_0)]$ and $\mathbf{n}_\perp = \nabla p/|\nabla p|$ is perpendicular to the confinement isobaric surfaces [27].

The total incident energy on the particle depends on its cross sectional area, while evaporation and re-radiation occurs on the hemispherical surface facing the plasma 'dayside', identified by the plane normal to $\mathbf{n}_q$.One can evaluate numerically a label for the illuminated particle hemisphere. At microscopic level the heat flux is transferred to the dust particles mainly by impinging plasma ions, which in general have a mean flow speed [12, 28],basically parallel to $\mathbf{b}$; the upstream heat influx, convective and diffusive, will exceed the downstream diffusive one. Regions not normal to incident heat flux are less heated and consequently re-radiation and evaporation is reduced by a cosine factor of the intrinsic polar angle [9]. For the present problem all the asymmetry effects can be summarized in a reduction factor ξ which models the anisotropic, fractional contribution [8–11, 29] of the sublimating/evaporating spherical half shell of thickness δ and volume $2\pi a_d^2 \delta$, which is assumed to be very small compared with the particle volume; hence $\xi \ll \frac{3\delta}{2a_d} \ll 1/2$, with outgassing expected around the direction $\mathbf{u} = \overline{O'M}/|\overline{O'M}|$, with reference to figure 1 and appendix A [8, 9, 11]. This approach is not in contradiction with the estimate worked out in [29] in a cruder slab geometry. The *asymmetric* mass outgassing from the dust particle surface, which in principle drives a rocket force, has three components: one along the direction

vector $\mathbf{n}_q$, another in the transverse direction vector $\mathbf{t}$ normal to $\mathbf{n}_q$ in the particle equatorial plane and the third $\mathbf{n}$ tangent to the trajectory [5, 6, 11]. The unit vector $\mathbf{u} = \overline{O'M}/|\overline{O'M}|$ in a direction of maximum outgassing, on the day-side, is determined by the three angles (I, η, ϕ) in the spherical dust intrinsic reference frame, and in the local frame associated with $\mathbf{n}_q$ it is expressed by the components [5, 11]:

$$u_{n_q} = -[\cos\eta + (1 - \cos\eta)\sin^2 I \sin^2\phi], \tag{11}$$

$$u_n = -[\sin\eta\cos I + (1 - \cos\eta)\sin^2 I \sin\phi\cos\phi], \tag{12}$$

$$u_t = -[\sin\eta\sin I\cos\phi - (1 - \cos\eta)\sin I\cos I\sin\phi]. \tag{13}$$

For the purpose of determining the direction of the rocket force in the point-like limit,it is not necessary to evaluate the heat flux on the dust surface as long as $q_\perp/q_\parallel \ll 1$. However significant deviations from the directions parallel to $\mathbf{B}$, due to $\mathbf{q}_\perp$ may occur in the tokamak divertor region; embedding the calculation in a numerical code which deals with the actual configuration and computes the heat flow to the dust particle adopting the acceped theories [12], automatically takes care of the problem. For the case of the dust grains, to leading order in η the equation (11) gives: $u_{n_q} = -1$, $u_n = 0$, $u_t = 0$. Therefore the direction vector of peak mass ejection at a Knudsen flow rate is $\overline{O'M}/|\overline{O'M}| \simeq -\mathbf{n}_q$.

5.2. Asymmetric mass ejection factor

Here we give a brief comment on he small factor ξ, [8, 9, 11], previoulsy introduced. With the 'comet' model the anisotropy of outgassing depends (through ξ) on the *geometrical* fraction of heated surface and on the depth of the evaporating layer, akin to the *'comet vent'* concept [8–10]. A self-consistent determination of the fractional asymmetric sublimation/evaporation factor ξ in expressions (14) and (15), even for a single, 'typical', particle or drop of a population, is not practically possible and useful, as it involves too many uncertain or inaccessible inputs, such as, for instance: deviation from sphericity (in flight), heat transmission across the particle volume, depth of ablated layer,deforming effects of reflecting impacts with the wall. A relatively simple *closure* condition which *could* be imposed to find an order of magnitude and a consistent ξ, is a careful heat flux balance, extending that of [9, 30, 31] to determine the small percentage difference between the lit side and unlit side pressures associated with the slightly different temperature, retaining also the important vector information on the rocket acceleration. However also this procedure would not improve significantly the evaluation of the effect, since a more general conclusion can be read from the scaling of the momentum flux rate equation (7) with ξ and $p_s(T_i^L)$ (see figure 4). It is clearly shown that for temperature above melting the acceleration exceeds gravitation even for very small values of ξ, whatever *the asymmetry mechanism might be*. Therefore more useful, unbiased information can be gotten,in the tests and applications, using ξ as a free parameter, within the range $0 < \xi \ll 1/2$, constant during the dust flight.

5.3. Scaling and direction of force and torque

From the previous sections the Tsiolkovski rocket force can be modeled in magnitude and direction,using expressions (8), (10). The scaling of the magnitude of $F_{\rm rock}$ can be obtained using equation (7). The dominant contribution to the rocket force on a spherical dust particle,due to evaporation/sublimation processes, can then be cast in the form:

$$\mathbf{F}_{\mathbf{rock}} = 2a_d^2\xi\hat{M}_{\rm Mach}p_s(T_i^L)H(s)\left(\frac{\mathbf{v}_{\mathbf{rel}}}{|v_{\rm rel}|}\cdot\mathbf{n}_q\right)\mathbf{n}_q\,. \tag{14}$$

Here H is the Heaviside function, vanishing for negative argument, switches from the 'dayside' to 'nightside' of the particle trajectory with respect to the plasma SOL,and where ξ indicates the effective, small, *asymmetric fraction* of particle surface ejecting mass [9, 11, 29].

Expression (14) incorporates the relevant component of the outgassing velocity relative to the C.M., $\mathbf{v}_{\mathbf{rel}}\cdot\mathbf{n}_q \simeq \frac{8}{9}\sqrt{\frac{RT_i^L}{2\pi M}}$ [19, 20]. The basic scaling and the order of magnitude of the rocket acceleration $a_{\rm rock}$, in the particle frame, is given by:

$$\frac{F_{\rm rock}}{M_d} = \frac{3\xi\hat{M}_{\rm Mach}}{2\pi a_d}\frac{p_s(T_i^L)}{\rho}. \tag{15}$$

From equations (9) we can estimate an orbital torque driving a rotation of a particle with CM at position $\mathbf{r} \equiv \mathbf{r}_{\rm CM}$, if unhindered by opposing viscous effects, with a rate:

$$\frac{{\rm d}\omega}{{\rm d}t} \approx \frac{15\xi\hat{M}_{\rm Mach}}{4\pi a_d^2\rho}p_s(T_i^L)\mathbf{r}_{\rm CM}\wedge\mathbf{n}_q. \tag{16}$$

Consequently the typical time scale for half revolution that swithches 'night-' with 'day-side' for a 100μ particle would be of the order of $t_\pi \simeq \frac{4\pi^2 a_d^2\rho}{15\xi\hat{M}_{Mach}p_s(T_i^L)}$, ranging from $\approx 10^{-3}$ s, for $\xi = 0.1$, $T_i^L = 1552\,^\circ$K to $\approx 10^{-5}$ s for $\xi = 0.1$, $T_i^L = 1850\,^\circ$K. This contributes to uniformization of the surface temperature, thereby canceling the rocket effect due to $\delta T \neq 0$, while a purely geometrical nonuniformity of heating, around the direction $\mathbf{n_q}$, could provide a 'comet vent' effect [8] maintaining the rocket effect. The dependence of the angular acceleration on temperature through $p_s(T_i^L)$ is strong, and the related size reduction due to mass loss (here not explicitely considered), can drive observable spinning and out-of-plane orbit deviations of the particles. This can be a help for understanding several observations [2], although it is well known that spinning of dust particulate can be due to numerous other effects, such as electric dipole forces [32, 33], or for conducting grains, $\mathbf{J}\wedge\mathbf{B}$ forces due to currents associated with different paths of magnetized impinging ions and electrons [29]. In any case it is expected that, in the denser SOL layers, any rotation driven by the 'rocket' and other torques be limited by viscous reaction of the surrounding plasma. All the quantities $(\mathbf{n}, \mathbf{n}_q, v_{\rm rel}, T_s^L, p_s, a_d, M_d)$ in expression (14) must be evaluated numerically, related to the plasma background and to the dust trajectory. Therefore with this procedure applicable to very small particles, the identification of the direction of the Tsiolkovski rocket force is obtained just with reference to the C.M. orbit and can be easily implemented in dust trajectory codes, (such as DUSTT [12, 13], DTOKS [34], MIGRAINe [35], DUSTTRACK [14]) which

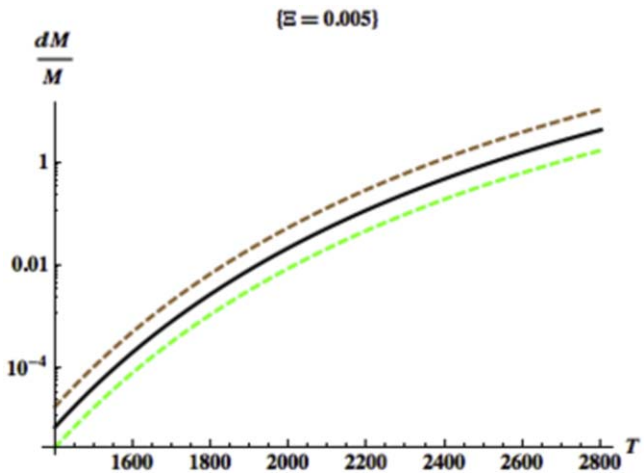

Figure 3. Percentage of mass loss/sec versus particle temperature, for Be particles of radii 40, 100, 250 μm and $\xi = 0.005$.

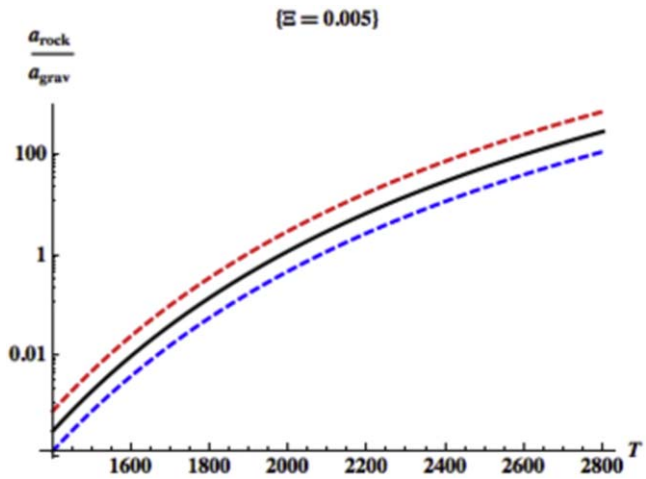

Figure 4. Ratio of rocket acceleration over gravitational (g) versus temperature for particles radii 40, 100, 250 μm with mass evaporation flux evaluated following [17, 20, 21] with $\xi = 0.005$.

calculate all the mechanical and thermodynamical evolution of isolated dust particles.In addition to the mechanics of motion, one should note that ablation has consequences also on the charge evolution and heat exchange,which are treated self consistently in the full tracing codes [12–14, 34, 35].

6. Numerical tests and examples

The relevance of the rocket acceleration on particulate mobilized in a tokamak vacuum chamber needs to be assessed by clear-cut examples, albeit in idealized situations. An example of this kind is proposed for the specific case of micrometric Be dust particles, assumed to be falling, in vacuum, under gravity from the top of a JET-like tokamak vessel. The first information is provided by figures 3 and 4 which show, for particles sizes $a_d = 40,\ 100,\ 250\ \mu$m, the relative mass loss rate and the expected rocket acceleration normalized on g, versus the particle initial surface temperature (just below melting point), assumed fixed. It is apparent that a mechanical description is meaningful in a temperature interval much below boiling temperature, $T_{\rm boil} = 2743$ °K, even for a very small ξ. An integration of equations (8), (9) in the main (R, ϕ, Z) coordinate system is performed comparing the case of free fall (in vacuum and with no magnetic field) with that including the rocket effect. The typical input data, in a JET-like geometrical domain, wth major radius $R_{ax} = 2.96$ m and vessel top $Z_{\rm up} = 1.8$ m, are reported in table 3. The dust trajectories in the (R, Z) plane with $T = 1552$ °K (sublimation range) are evaluated deliberately with extreme values of the asymmetric emission factor values $\xi = 0.005$, and $\xi = 0.5$, which is the theoretical maximum. Incidentally,a realistic situation in which $\xi \simeq 0.5$ could be that of a composite dust material, with different evaporation energies [29], but this is not actually an objective of this work. A first test is performed with the free fall trajectory of a 100μ Be particle at $T = 1552$°K, starting from ($R = 2.21$ m, $Z = 1.7$ m). The comparison with that modified by the rocket force shows that at this temperature, the sensitivity to the mass asymmetric

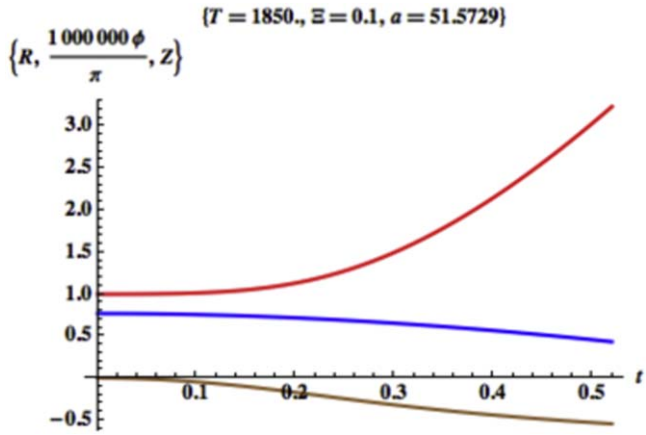

Figure 5. Evolution of (R, ϕ, Z) versus time with $\xi = 0.1$, and $T = 1850$ °K: the orbit deviates radially (R, red line. Z, blue line) and is (slightly) twisted ($10^6\phi/\pi$, brown line).

Table 3. Initial conditions for Be dust trajectories.

a_d (m)	T_i^L (°K)	$V_{\rm out}$ (m s^{-1})	R_0 (m)	Z_0 (m)	ξ
10^{-4}	1552	424	2.21	1.70	1×10^{-2}
		424	2.21	1.70	5×10^{-2}
		424	2.21	1.70	1×10^{-1}

ejection fraction ξ, in the range $0.005 < \xi < 0.5$, of the deviation from vertical is totally negligible and we omit displaying the figures. For a test case with surface temperature $T = 1850$ °K (molten state below boiling), the trajectories are displayed in figures 5 and 6 which show a first non negligible deviation with $\xi = 0.1$, with slight orbital twist (figure 5)and a dramatic flip of direction for the limiting value $\xi = 0.5$.

In conclusion, the orbit deviation, in the R direction,from the free fall direction is therefore generally very small for the range of temperatures and ξ values considered reasonable (i.e.

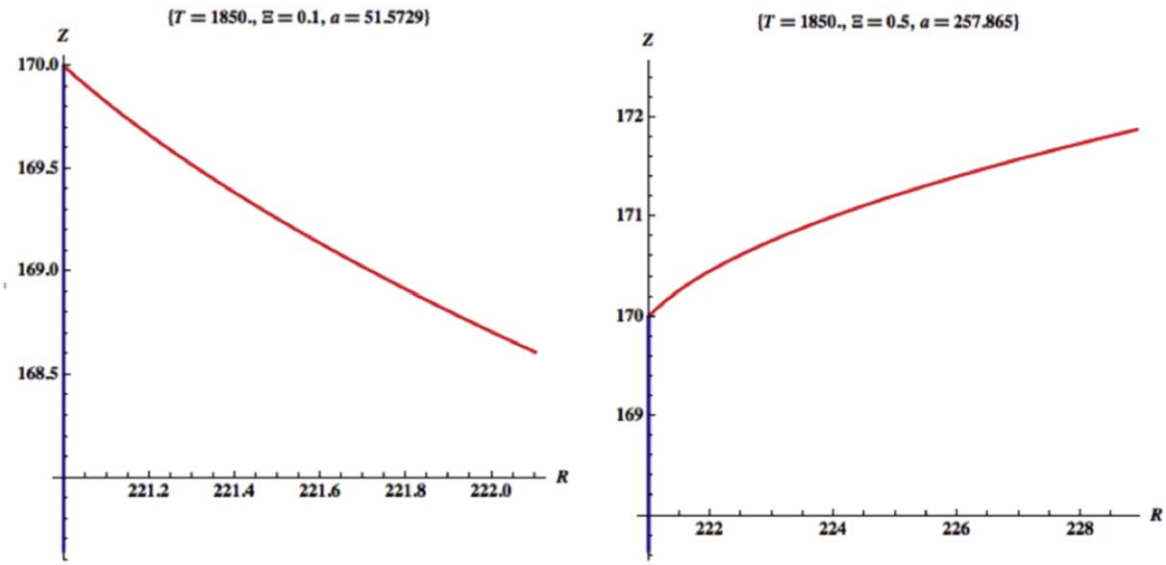

Figure 6. Response of trajectories in *RZ* plane of a 100μ Be dust grain to the mass ejection factor ξ, at $T = 1850$ °K (molten state). At this temperature in the range $0.1 < \xi < 0.5$, starting from ($R = 2.21$ m, $Z = 1.7$ m), the deviation due to the rocket acceleration (red) is significant and at higher ξ it flips upwards, against gravity.

Table 4. Accelerations compared to g.

a_d (m)	$T_{i,e}$ (eV)	t_{flight} (ms)	a_{drag}/g (m s^{-2})	a_{rock}/g (m s^{-2})	ξ
10^{-6}	10	1.6	$\simeq$5.5	100-12-0.05	0.1
5.5×10^{-6}		0.8	$\simeq$0.6	10-2-0.007	0.1
10^{-5}		0.6	$\simeq$0.25	10-1.5	0.1
10^{-6}	10	0.9	$\simeq$5.5	100-12-0.05	−0.1
5.5×10^{-6}		0.6	$\simeq$0.6	10-2-0.007	−0.1
10^{-5}		0.7	$\simeq$0.25	10-1.5	− 0.1

Table 5. Dynamic range of Be rocket effect.

a_d (m)	T_i^L (°K)	a_{rock} (m s^{-2})	$\omega(t = 0.1)$(rad s^{-1})	ξ
10^{-4}	1552	0.047	$\approx 10^2$	5×10^{-3}
	1552	0.95	$\approx 10^3$	1×10^{-1}
	1850	2.58	$\approx 1.2 \times 10^5$	1×10^{-1}
	1850	51.7		5×10^{-1}
	2400	294		5×10^{-3}

below boiling point), but increases significantly in response to the dust surface temperature, because of equation (7). A second numerical investigation is performed using the code DUST-TRACK [14], considering the full evolution of Be droplets with $T_d = 1560$ (°K) ejected from the top (upper dump plates) in a JET-like configuration and traveling in a fictitious, tenuous uniform plasma SOL ($n_e = n_i = 10^{18}$ m^{-3}, $T_e = T_i = 10$ eV, $V_{i,\phi} = -40$ m s^{-1}, $V_Z = -1$ m s^{-1}, with a magnetic field $B = 2$ T), under gravity and with inclusion of an *artificial* toroidal viscous drag, for a small range of drag acceleration around g, to test qualitative effects on particle trajectories, with and without rocket force. It is shown in the summary of tables 4 and 5 that the acceleration due to mass loss can significantly exceed gravity, if the surface temperature is on the high side of the melting point, but it is negligible at lower temperatures. Thus, a few particular examples can shed light on the general phenomenon and can be orient the interpretation of observations. Here we extend the conventions on ξ, attaching the sign of the launching velocity. In table 4 the quantitative comparison of is reported,of the acceleration due to viscous drag [12, 28] with the rocket one, during 'test" flights of different duration. For both $\xi > 0$ and $\xi < 0$ the magnitude of rocket acceleration drops in one or two time steps within a flight time,which is shorter for $\xi < 0$ (the sign of ξ indicates just the direction of ejection, *chosen for test purposes*). In table 5 an example of the dynamic range of the rocket effect for a 100μ Be particle is displayed for

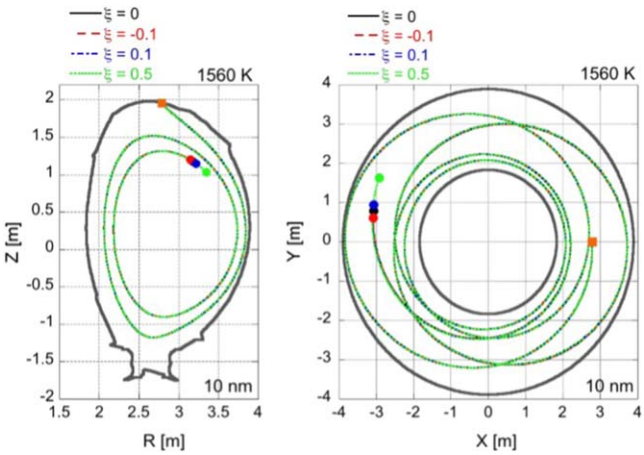

Figure 7. *RZ*, *XY* projections of dust trajectories calculated by DUSTTRACK [14], starting from ($R = 2.786$ m, $Z = 1.96$ m) Be droplets with $a_d = 10^{-8}$(m), $T = 1560$ °K subject to gravity and (artificial) SOL interaction, in presence of B field and $\xi = 0, -0.1, +0.1, +0.5$.

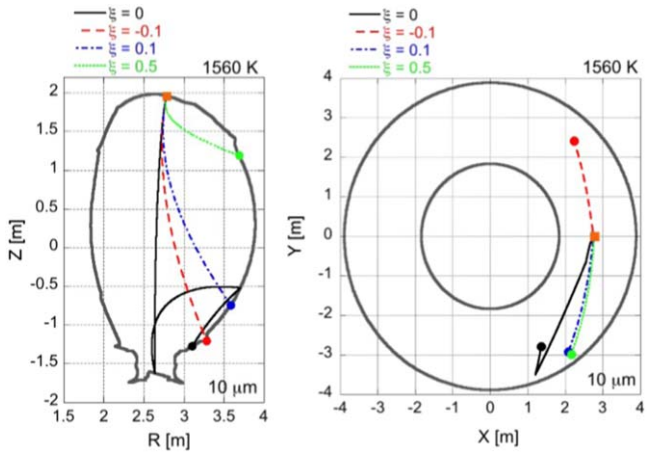

Figure 8. *RZ*, *XY* projections of dust trajectories calculated by DUSTTRACK [14], starting from ($R = 2.786$ m, $Z = 1.96$ m) Be droplets with $a_d = 10^{-5}$ (m), $T = 1560$ °K subject to gravity and (artificial) SOL interaction, in presence of B field and $\xi = 0, -0.1, +0.1, +0.5$.

different surface temperatures and (assumed) ξ factors. It is clear that above melting the acceleration and the spinning of a drop grow to values where other physical effects, should be taken into account,expected to lead to destruction of the integrity of a finite particle and consequently of the point-like limit model. The model holds up to the point where the nominal radius of the evaporating particle reaches the slowing down distance of incident plasma ions [12]; this situations opens up new scenarios and problems outside the present context. The first case in figure 7 shows the trajectories in the meridian and equatorial planes of very small ($a_d = 10$ nm) particles, with three values of mass ejection fraction: $\xi = 0$ (no rocket effect), and $\xi = \pm 0.1$, and $\xi = 0.5$ (see figure captions). It is apparent that in a case like this the rocket acceleration has a negligible effect, even in comparison with the effect of the Lorentz force.

If the rocket acceleration is included in the dynamics, albeit with a very small asymmetric mass loss, it appears that the trajectory can be strongly modified following the surface temperature evolution, exhibiting even a 'firework' behavior, often observed in experiments [2]. The first figure, 7 shows, for $\xi = 0, -0.1, +0.1, +0.5$ the typical trajectories subject to gravity and wall reflections, and in presence of the tokamak magnetic field, which affects just the motion of the smallest particle: the very lightest one ($a_d \simeq 10^{-8}$ m) tends to cling to the outer wall and eventually it travels around the full torus in the equatorial plane. The effect of the rocket force, assumed here for simplicity to be directed along $\mathbf{n_q} \simeq \mathbf{e}_\phi$ is displayed in the next figure 8 for $a_d = 10^{-5}$(m) and $\xi = 0, -0.1, +0.1, +0.5$. The finite deviation toward the low field side is evident for the heavier particles. In figure 9 the similar trajectory is evaluated for mass ejection for $a_d = 10^{-4}$(m) and $\xi = 0, -0.1, +0.1, +0.5$. *A posteriori* it can be concluded from these tests and the previous theory, that the modest sensitivty of the acceleration to ξ, due to the high sensitivity to temperature, justifies taking is as constant during a flight time.

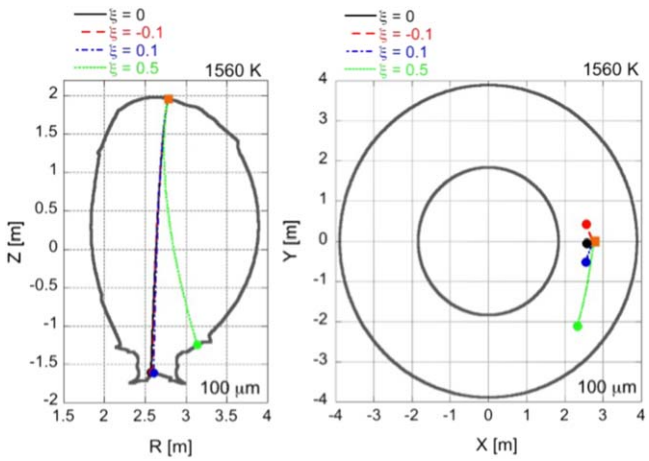

Figure 9. *RZ*, *XY* projections of dust trajectories calculated by DUSTTRACK [14], starting from ($R = 2.786$ m, $Z = 1.96$ m) Be droplets with $a_d = 10^{-4}$ (m), $T = 1560$ °K subject to gravity and (artificial) SOL interaction, in presence of B field and $\xi = 0, -0.1, +0.1, +0.5$.

7. Conclusions

The assessment of the effects of *asymmetric mass loss* of dust particles on their flight trajectories in the SOL of a tokamak requires finding the scalar and vector characteristics of the *Ziolkowsky* type rocket force. This classical dynamical problem is not trivially simple even in vacuum,due to the nonlinear process of heating and evaporation, and it cannot be formally solved self-consistently, but paradigmatic examples can lead to a formulation applicable to studies of interaction with the plasma SOL. This short work discusses from first principles a simple reduction to a point-like approximation model of a particle which loses mass, relying just on the C.M. trajectory in the SOL, with non uniform temperature. The asymmetry of mass ejection is related to the persistent direction of the heat flux, mainly due to impinging ions,

different from that of the C.M. trajectory. The scaling of the Ziolkovski acceleration with temperature leads to the important conclusion that above melting it can exceed gravity *regardless* of the details of the asymmetric ejection. The model is easily applicable to current numerical codes [12, 14, 34, 35] which evaluate the mechanical and thermodynamical evolution of dust particles in realistic tokamak geometry. The main result is the assessment of the vector and scalar aspects of the rocket force, its scaling with particle size, surface temperature and the comparison with gravity. Exemplary tests are provided to show the important qualitative effects on the trajectories. The tests lead also to establish the limits of a point-like model.The effect explored can be significant if the dust temperature is close to melting, in the extreme scenarios of disruptions and in special regions of the tokamak,such as the divertor throat.

Acknowledgments

This work has been carried out within the framework of the EUROfusion Consortium and has received funding from the Euratom research and training programme 2014–2018 and 2019–2020 under grant agreement No. 633053. The views and opinions expressed herein do not necessarily reflect those of the European Commission.

Appendix A. Geometry

In the particle intrisic frame (figure 1)(O', $\mathbf{e}_1$, $\mathbf{e}_2$, $\mathbf{e}_3$), O' is the center of the particle core, the axis $\overline{O'P}$ is toward the 'north pole' and here is assumed aligned with the tangent to the particle trajectory, i.e. parallel to the CM velocity direction $\mathbf{n} = \mathbf{v}_{\rm CM}/v_{\rm CM}$; $\mathbf{r}(\mathbf{t})_{\rm CM} = \overline{OO'}$ is the trajectory of the CM; the axis $\overline{O'R}$ and the unit vector $\mathbf{e}_\Omega$ represent the instantadeous spinning axis; the points S and M on the (spherical) surface indicate *generic* points of peak heat absorption and mass sublimation, respectively. The illuminated region is upstream of a plane perpendicular to $\mathbf{n}_q$. In principle there is an angular lag angle $\boldsymbol{\eta}$ between the meridians of M and S. In order to take advantage of the procedure of [5, 6, 11], in principle a rotation axis different from $\overline{O'P}$ should be considered,with an obliquity angle I with respect to $\overline{O'P}$. However here we shall consider η a small parameter so that $\overline{O'M} = \overline{O'S} + \eta\frac{\partial\overline{O'S}}{\partial\eta} + O(\eta^2)$, and look for a formulation where it vanishes. In this limit the fixed obliquity angle plays no role. The lag angle η between the 'hotspot" S and the peak mass ejection spot M can be considered proportional to the heat diffusion time $\tau_T \simeq \frac{\delta^2}{\kappa_T} \ll \frac{a_d^2}{\kappa_T}$ in the heated layer of thickness $\delta \ll a_d$. Then applying dimensional analys is to $\frac{{\rm d}T}{{\rm d}t} = \kappa_T\nabla^2 T$, we estimate $\eta = O(\delta^2)$ and becomes negligible in the small particle limit. In the limit condition of free fall in very tenuous plasma, $\mathbf{n} \longrightarrow \mathbf{e}_Z$, $\mathbf{n}_q \longrightarrow \mathbf{b} = \mathbf{e}_\phi + \frac{B_\theta}{B_\phi}\mathbf{e}_\theta$ and the rocket acceleration is expected to be reduced since $\mathbf{v}_{\rm rel}\cdot\mathbf{n}_q \approx v_{\rm rel}\frac{B_\theta}{B_\phi}\mathbf{e}_\theta.\mathbf{e}_Z$.

Appendix B. Formulae and units

For convenience of the interested reader, we collect here the basic notions, symbols and data about mass evaporation/sublimation, in consistent units, as used in this work.

B.1. Basic definitions and conventions and units [17, 18, 20, 21]

Atomic mass unit (Dalton): $m_{\rm au} = 1.660\,539\,040(20) \times 10^{-27}$ (kg)

Atomic (molecular) mass of gas: m (kg)
Relative atomic (molecular) mass (or *weight*): m_a read or constructed from Mendeleev table
Molar mass: M mass (grams) of 1 mole of substance = relative atomic mass $\times$(1 g mol^{-1})
n(mol) = m(kg)/M(kg mol^{-1}): amount of substance in SI units = number of moles $N = nN_{\rm A}$: number of gas molecules

$$N_{\rm A} = 6.022 \times 10^{23}, \tag{B1}$$

$$m_{\rm au}(1\ {\rm Dalton}) = 1.66 \times 10^{-27}({\rm kg}) \equiv \frac{10^{-3}}{N_{\rm A}} \quad ({\rm kg}), \tag{B2}$$

$$m = m_a \times m_{\rm au} = \frac{M}{N_{\rm A}}, \tag{B3}$$

$$M = m_a \times 10^{-3} \quad ({\rm kg\ mole}^{-1}), \tag{B4}$$

$$R = N_{\rm A}k_B = 8.314\,4598 \quad ({\rm kg\ m^2\ s^{-2}\ {}^\circ K^1\ mol^{-1}}), \tag{B5}$$

$$\widehat{R} = \frac{R}{M}. \tag{B6}$$

For the particular case of Beryllium, considered in this work, the data are:

$$m_{\rm Be} = 9.012 \tag{B7}$$

$$m = m_{\rm Be} \times m_{\rm au} = \frac{9.012_{\rm Be} \times 10^{-3}}{N_A} \quad ({\rm kg}) \tag{B8}$$

$$M = m_{\rm Be} \times 10^{-3} \quad ({\rm kg\ mole}^{-1}) \tag{B9}$$

$$\widehat{R} = \frac{R}{M} = 922.59 \quad ({\rm m^2\ s^{-2}\ {}^\circ K^{-1}})]. \tag{B10}$$

The units used here for other fundamental quantities are : temperature T (°K), vapor pressure p_v (Pa). The essential form of the ideal gas law is $pV = nRT = Nk_BT$. In the formulation of [17] the gas constant is replaced by the reduced constant $\widehat{R} = R/M$ (J °K^{-1} kg^{-1}) and the gas law is rewritten as $p = \frac{m}{V}\widehat{R}T = \rho\widehat{R}T$. In the context of evaporation/sublimation the vapor density and vapor velocity and pressure can be re-expressed in terms of the (sublimation/vaporization) temperature as $\rho_v = \frac{p_v}{\widehat{R}T_v}$ (kg m^{-3}) and $v_{\rm th} = \sqrt{2\widehat{R}T_v}$ and $p_v = \frac{\rho}{2}v_{\rm th}^2$ [17]. According to [18, 20] the mean ejection velocity can be estimated as $V_{\rm out} \simeq \frac{8}{9}\sqrt{\widehat{R}T_v/2\pi}$.

Table B1. Test cases with Beryllium.

T_v(K)	ρ_v(kg m^{-3})	p_v(Pa)	$u_g = \frac{8}{9}\sqrt{\frac{\widehat{R}T_L}{2\pi}}$ (m s^{-1})	$a_{\rm rock}/g$
1552	3.225×10^{-6}	4.62	424	0.06
3243	1.39×10^{-3}	4.18×10^{3}	613	5.5

B.2. Comparison of various expressions of evaporation/ sublimation fluxes

Here we compare various expressions for the flux of evaporated mass,with the convention of assuming the *accomodation factor* [15, 18–21] $\alpha = 1$:

$$\Gamma_{EU_m} = p_v\sqrt{\frac{1}{2\pi\widehat{R}T}}. \tag{B11}$$

The particle number flux is obtained dividing equation (B11) by the molecular mass $m = M/N_{\rm A}$, equation (B3):

$$\Gamma_{EU_n} = \frac{p_v N_{\rm A}}{\sqrt{2\pi MRT}} = \frac{2.6347 \times 10^{24} p_v}{\sqrt{m_a T}} \quad ((n.\text{particles})\,\text{m}^{-2}\,\text{s}^{-1}) \tag{B12}$$

The Holyst expression for the particle number flux [21] is analogous to B12:

$$\Gamma_{LV} = \alpha\frac{p_L}{\sqrt{2\pi m k_B T_i^L}} \quad ((n.\text{particles})\,\text{m}^{-2}\,\text{s}^{-1}). \tag{B13}$$

A classical reference, used here to benchmark the calculations is the paper by Holden *et al*, [15] on the evaluation of the vapor pressure of Be. There the following expression is used , in cgs units:

$$\Gamma_{\rm Hold} = p(\text{atm})\sqrt{\frac{M(\text{g mol}^{-1})}{2\pi R(\text{erg °K}^{-1}\text{mol}^{-1})T(\text{°K})}} \quad (\text{g cm}^{-2}\,\text{s}^{-1}). \tag{B14}$$

A test of the present calculations against [15] is shown in figure 2 which displays the mass flux in (g cm^{-2} s^{-1}) in the temperature range $1100 < T < 1600$, used in [15]. From equation (B11) the Hertz–Knudsen mass flux (kg m^{-2} s^{-1}) can be also expressed in the alternative (Cercignani [17]) form:

$$\Gamma_{Kn_m} = \rho_v\sqrt{\frac{\widehat{R}T_v}{2\pi}} = \rho_v u_g. \tag{B15}$$

B.3. Properties of Beryllium

Solid density $\rho_s = 1842$(kg m^{-3}), liquid density $\rho_L = 1690$ (kg m^{-3}), melting temperature (solid–liquid) $T_f = 1560$ (°K), boiling temperature (liquid-vapor) $T_b = 2742$(°K). A summary of values of rocket acceleration for typical Be thermodynamical states is given in table B1.

ORCID iDs

E Lazzaro https://orcid.org/0000-0002-3291-8890
A Uccello https://orcid.org/0000-0003-3044-1715

References

[1] Widdowson A, Alves E, Ayres C F, Baron-Wiechec A, Brezinsek S, Coadd J P, Heinola K, Likonen J, Matthews G F, Rubel M and JET-EFDA contributors *Proceed of 14th Int. Conf. on Plasma Faciing Materiialls and Components Juelich, 13-17 May 2013, Material Migration Patterns and Overview of First Surface Analysis of the JET ITER-likeWall, bfI15, 27*
[2] Flanagan J C *et al* 2015 *Plasma Phys. Control. Fusion* **57** 014037
[3] Matthews G F *et al* 2016 *Phys. Scr.* **T16** 014070
[4] Litaudon X *et al* 2017 *NF* **57** 102001
[5] Sekanina Z 1979 *Icarus* **37** 420
[6] Sekanina Z 1981 *Ann. Rev. Earth Planet. Sci.* **9** 113–45
[7] Sekanina Z 1987 *Anisotropic Emission from Comets: Fans Versus Jets: I. Concept and Modeling, in Diversity and Similarity of Comets* ed E J Rolfe and B Battrick (Eur. Space Agency Spec. Publ.) pp 315–22 ESA-SP 278
[8] Sekanina Z 1988 *Astron. J* **96** 1456
[9] Wallis M K and Macpherson A K 1981 *Astronom. Astrophys.* **98** 45–9
[10] Kelley M C *et al* 2013 *Icarus* **222** 634–52
[11] Yeomans D K 1994 *Asteroids, Comets, Meteors 1993 (Proceedings of the 160th Symposium of the International Astronomical Union held in Belgirate,Italy, June 14-18, 1993.)* ed A Milani, M Martino Di and A Cellino (Dordrecht: Kluwer Academic Publishers) pp. 241–54
[12] Pigarov A Y *et al* 2005 *Phys. Plasmas* **12** 122508
[13] Krasheninnikov S I, Smirnov R D and Rudakov D L 2011 *Plasma Phys. Control. Fusion* **53** 083001
[14] Gervasini G, Lazzaro E and Uccello A 2017 *J Fusion Energy, J Fusion Energy* **36** 25
[15] Holden R, Speiser R and Johnston H 1948 *J. Am. Chem. Soc.* **1** 3897
[16] Alcock C B, Itkin V P and HorriganCanadian M K 1984 *Metall. Quartely* **23** 309
[17] Cercignani C 2000 *Rarefied Gas Dynamics,* (Cambridge: Cambridge University Press) ch 8
[18] Bond M and Struchtrup H 2004 *Phys. Rev.* E **50** 061605
[19] Barrett J and Clement C 1992 *J. Colloid Interface Sci.* **150** 352–64
[20] Safarian J and Engh T A 2012 *Metall. Mater. Trans.* A **44A** 747
[21] Holyst R, Litniewsky M and Jakubsczyk D 2015 *Soft Matter* **11** 7201–6
[22] Persad A H and Ward C A 2016 *Chem. Rev.* **116** 7727–67
[23] Ytrehus T 1983 *Phys. Fluids* **26** 939
[24] Muratova T M and Labuntsov D A 1969 *High Temp.* **7** 888–96
[25] Holyst R and Litniewsky M 2009 *J. Chem. Phys.* **130** 074707

[26] Plastino A R and Muzzio J C 1992 *Celestial Mechanics and Dynamical Astronomy* 53 (Netherlands: Kluwer Academic Publishers)
[27] Hazeltine R D and Meiss J D 1992 *Plasma Confinement* (Redwood City: Addison-Wesley Publishing Company)
[28] Chandrasekhar S 1943 *Astrophys. J.* **97** 255
[29] Krasheninnikov S I, Pigarov A Y, Smirnov R D and Soboleva T K 2010 *Contrib. Plasma Phys.* **50** 410– 425
[30] Guettler C *et al* 2017 *Mon. Not. R. Astron. Soc.* **469** S312
[31] Krieger K *et al* 2011 *Phys. Scr.* **T145** 014067
[32] Shukla P K 2001 *Phys. Plasmas* **8** 1791
[33] Krasheninnikov S I, Shevchenko V I and Shukla P K 2007 *Phys. Lett.* A **361** 133–5
[34] Bacharis M, Coppins M and Allen J E 2010 *Phys. Rev.* E **12** 026403
[35] Ratynskaia L V S, Tolias P, Bykov I, Bergsåker H, Litnovsky A, den Harder N and Lazzaro E 2013 *Nucl. Fusion* **53** 123002